Book of Tutorials and Abstracts

European Microbeam Analysis Society

EMAS 2023

17th

EUROPEAN WORKSHOP

on

MODERN DEVELOPMENTS AND APPLICATIONS IN MICROBEAM ANALYSIS

7 to 11 May 2023
at the
Jagiellonian University, Auditorium Maximum
Krakow, Poland

Under the auspices of the Rector of the
Jagiellonian University, Krakow, Poland
Organised in collaboration with the
Institute of Metallurgy and Materials Science of
the Polish Academy of Sciences, Krakow, Poland

EMAS
European Microbeam Analysis Society eV
www.microbeamanalysis.eu/

This volume is published by:
European Microbeam Analysis Society eV (EMAS)
EMAS Secretariat
c/o Eidgenössische Technische Hochschule, Institut für Geochemie und Petrologie
Clausiusstrasse 25
8092 Zürich
Switzerland

ISBN 978 90 8227 6961
NUR code: 972 – Materials Science

SOFT X-RAY EPMA: CHOOSING THE RIGHT MACs

X. Llovet[1], P. Pöml[2], A. Moy[3] and J.H. Fournelle[3]

1 Universitat de Barcelona, Centres Científics i Tecnològics (CCiTUB)
C/ Lluís Solé i Sabarís, 1-3,08028 Barcelona, Spain
2 European Commission, JRC Directorate G - Nuclear Safety and Security
P.O. Box 2340, 76125 Karlsruhe, Germany
3 University of Wisconsin, Department of Geoscience
US-53706 Madison, WI, U.S.A.
e-mail: xavier@ccit.ub.edu

Xavier Llovet runs the electron microprobe laboratory at the University of Barcelona, where he has worked since 1991. He received his PhD in physics from the University of Barcelona in 1998 and was awarded the accreditation of research by AQU Catalonia in 2010. His research interests include electron probe microanalysis methods, X-ray spectrometry and Monte Carlo simulation of electron-beam interactions. He has contributed to over 95 peer-reviewed publications and has given multiple invited lectures at international meetings. He has been guest editor of the journals Microchimica Acta and IOP Conference Series: Materials Sciences and Engineering on several occasions. He is Board member (1999-2019; 2022-) and served as Vice-president (2012-2019) of the European Microbeam Analysis Society (EMAS). He received the Cosslett Award from the Microanalysis Society of America (MAS) in 2005 and 2014 and the EMAS Medal for Services to the Society in 2019.

1. ABSTRACT

The use of soft X-rays for electron probe microanalysis (EPMA) has gained widespread interest over the past decades. Because X-ray absorption is the dominant correction for soft X-rays, a reliable set of mass attenuation coefficients is needed for accurate composition determination. In this paper, we attempt to examine the current situation of mass attenuation coefficients for soft X-rays in the context of EPMA.

2. INTRODUCTION

Over the past decades, electron probe microanalysis (EPMA) has moved forward with a combination of technical developments, allowing advances in measurements of soft X-rays (< 1 keV photon energy) [1]. Such X-rays are used for the analysis of the light elements (Li, Be, B, C, N, O, and F), which often play a critical role in the properties of many materials. Falling also within the soft X-ray region are the L-lines of medium atomic number (Z) elements such as the first-row transition metals (Sc to Cu) and the M-lines of high-Z elements such as the rare-earth elements. These X-ray lines are needed for the analysis of natural and technological materials that are heterogeneous on a sub-micrometre scale, which require the operation of the EPMA at low accelerating voltage [1].

Soft X-rays are produced in electron transitions involving valence electrons, which are affected by chemical bonding. Thus, soft X-rays can reveal details of the chemical bonding state of an atom. For example, the L-lines of transition metals, which originate from the transition from the 3d valence level to the 2p core level, provide information on the electronic structure of many materials [2]. However, because of that, the use of soft X-rays for elemental analysis often results in large errors in the evaluated concentrations, since matrix corrections do not include corrections for bonding effects (see e.g., [3-5]). One of the difficulties in using soft X-rays for microanalysis is the lack of accurate mass attenuation coefficients (MAC) that are required to correct for absorption effects within the specimen. For soft X-rays, MACs are generally of the order of several thousand cm^2/g, making X-ray absorption the dominant matrix correction. Actually, none of the existing matrix corrections programmes can provide accurate EPMA concentrations without a set of reliable MACs. In this sense, it has been emphasised that for soft X-rays an uncertainty in the MAC of 1 % commonly leads to a relative error of 1 % in the concentration [6].

Different MAC datasets are currently available in EPMA software packages, which cover the EPMA range of interest down to ~ 100 eV. These datasets consist of tabulated values for the most commonly used X-ray lines and emitter-absorber pairs. However, the accuracy of the different MAC datasets is poorly documented and one often finds that different MAC datasets produce significant differences in results. Moreover, because of their different nature, it is unclear whether the newer databases should replace the older ones, particularly where specific

EPMA matrix corrections might have had internal parameters fine-tuned based upon a particular MAC dataset. In this paper, we review the current situation of MACs for soft X-rays in the context of EPMA. We focus on the K-lines of the ultra-light elements (Be, B, C, N, O, and F), giving special attention to the actinide absorbers, and on the L-lines of first-row transition metals, where the difficulties arise from the proximity of the X-ray emission lines to the absorption edges. Finally, the situation of ultra-soft X-rays is briefly discussed.

3. MASS ATTENUATION COEFFICIENT DATASETS

One of the most popular source of MACs in EPMA is the 1986 analytical expression of Heinrich [7] (referred hereafter as Heinrich86), which was obtained from fits to experimental data. In the soft X-ray region, because of the lack of experimental information, the theoretical predictions of Veigele [8] were used, in combination with a few available measurements. The uncertainties in Heinrich86 MACs are estimated at 5 %, except for energies below 800 eV and regions close or between absorption edges, which are much larger, not being recommended for photon energies below 180 eV [7]. Heinrich86's MACs are also known as the MAC30 compilation.

Another source of MACs for soft X-rays is the semi-empirical tabulation of Henke *et al.* [9] (hereafter referred to as Henke82). Henke82's MACs, which covers the range from 30 eV to 19 keV and Z = 1 to 94, are mainly based on the experimental data available in 1982. Because for many elements there was little or no published experimental data, Henke *et al.* relied on theoretical calculations to interpolate and extrapolate across Z to fill the empty gaps. The theoretical calculations were also used to average the near-edge fine structure in the μ/ρ-curves. In 1993, Henke *et al.* [10] revised and extended their 1982 tabulation by including new experimental data and used new theoretical calculations to establish consistency through all values of Z. The 1993 Henke tabulation (hereafter referred to as Henke93) covers the energies from 50 eV to 30 keV and elements with Z = 1 to 92.

From the theoretical point of view, μ/ρ can be calculated as

$$\left(\frac{\mu}{\rho}\right) = \frac{N_{\mathrm{A}}}{A_{\mathrm{M}}}\left(\sigma_{\mathrm{ph}} + \sigma_{\mathrm{Co}} + \sigma_{\mathrm{Ra}}\right) \tag{1}$$

where N_{A} is Avogrado's number, A_{M} is the molar mass of the compound, and σ_{ph}, σ_{Co} and σ_{Ra} are the cross-sections for photo-absorption, Compton scattering and Rayleigh scattering, respectively. For photon energies below ~ 1 keV, photo-absorption absorption dominates Compton and Rayleigh scattering and μ/ρ can be approximated as

$$\left(\frac{\mu}{\rho}\right) \sim \frac{N_{\mathrm{A}}}{A_{\mathrm{M}}}\sigma_{\mathrm{ph}} \tag{2}$$

For instance, for uranium, the difference between the value of μ/ρ obtained by using Eq. (1) and that obtained by using Eq. (2) amounts to ~ 0.01 % at the O K-line energy (524.9 eV).

To calculate the photo-absorption cross-section for a compound the additivity rule is generally used, which states that any molecular cross-section can be obtained as the sum of the atomic cross-sections of the constituent atoms, thus neglecting chemical binding effects. Using the additivity rule, the MAC of a compound can be calculated as [11]:

$$\left(\frac{\mu}{\rho}\right) = \sum_i c_i \left(\frac{\mu}{\rho}\right)_i \tag{3}$$

where $(\mu/\rho)_i$ and c_i are the MAC and mass fraction of element i, respectively.

Different tabulations of theoretical photo-absorption cross-sections σ_{ph} are available in the literature. Chantler *et al.* [12] calculated photo-ionisation cross-sections for Z = 1 to 92 for photon energies over the range from 1 - 10 eV to 400 - 1,000 keV. The same author tabulated MACs near absorption edges for soft X-rays in the photon range from 100 eV to 10 keV for elements Z = 30 – 36 and Z = 60 - 89 [13]. Chantler's MACs are available from the National Institute of Standards and Technology (NIST) as the FFAST tabulation [14] and have been incorporated in most EPMA software packages. More recently, Sabbatucci and Salvat [15] calculated photo-absorption cross-sections for the inner subshells (up to the N_7 sub-shell) of elements Z = 1 to 99, for photon energies from the ionisation threshold up to 1 GeV. Sabbatucci and Salvat's photo-absorption cross-sections are implemented in the computer code PHOTACS [15]. Additional effects such as excitations to bound levels, finite life effects of the excited states and Pratt's screening renormalisation correction, can also be accounted for. Sabbatucci-Salvat cross-sections have been incorporated in the Monte Carlo simulation programme PENEPMA [16] as well as in the EPMA programmes BADGERFILM [18] and NIST DTSA-II [17].

4. MEASUREMENTS OF MASS ATTENUATION COEFFICIENTS

MACs can be experimentally determined by measuring the X-ray intensity, I, transmitted through a layer of an absorber element of mass thickness ρt by using the relation:

$$\left(\frac{\mu}{\rho}\right) = -\frac{1}{\rho t} \ln \frac{I}{I_0} \tag{4}$$

where I_0 is the intensity of the incident photon beam. Measurements for soft X-rays require the use of very thin solid films, whose thickness is difficult to determine accurately, and thus the experimental data may have limited accuracy in the soft X-ray region. In 1988, Saloman *et al.* [19] compiled the experimental X-ray attenuation cross-sections from papers that were published prior to 1988, which include the soft X-ray energy range 0.1 - 1 keV. Most of the measurements compiled by Saloman *et al.* were actually carried out in the 1960s and 1970s; from 1988 onwards very few measurements have been reported, with the exception of those performed by an international initiative group coordinated by standards laboratories in France, Germany, and other countries [20].

Attempts have also been made to determine the MACs from electron microprobe measurements (which have often been referred to as empirical MACs [21]). Kyser [22] determined the MACs for the Lα-lines of transition metals taking advantage of the relationship that exists between the MAC and the electron beam energy that produces the maximum X-ray intensity. Bastin and Heijligers made systematic determinations of MACs for the B-, C-, N- and O-Kα lines for a wide range of absorbers spanning the periodic table, which were published over the years in different reports [6, 23-25]. For a given specimen, these authors measured the element *k*-ratio at varying accelerating voltages and fitted the MAC such that the average k_{cal} / k_{exp} ratio, where k_{cal} and k_{exp} are the calculated and experimental *k*-ratios, respectively, yielded a value close to 1.

Pouchou and Pichoir developed a method to determine the MAC that requires the measurement and calculation of the emerging X-ray intensity from a sample of known composition at varying electron energies [26]. (μ/ρ) is then obtained by minimising the sum *S* of the quadratic deviations [26]

$$S = \sum_{k} \{\alpha\, I_{i,\mathrm{exp}}(E_k) - I_{i,\mathrm{th}}(E_k, (\mu/\rho))\}^2 \qquad (5)$$

where $I_{i,,exp}(E_k)$ and $I_{i,th}(E_k)$ are the measured and calculated X-ray intensities at incident electron energy E_k, respectively, and σ is a normalisation constant. Values of σ and (μ/ρ) are obtained by solving numerically the equations $dS/d\alpha = 0$ and $dS/d(\mu/\rho) = 0$. The developed method was implemented in the XMAC programme [4], which solves Eq. (5) iteratively by using the XPP model [27]. Using their method, Pouchou and Pichoir obtained the MACs for selected X-ray lines and absorbing elements [26], with an uncertainty that was estimated at ~ 5%. We note that to achieve such accuracy, consistent X-ray intensity measurements as a function of beam voltage need to be performed and, therefore, care has to be exercised to ensure instrument stability. Besides, both accelerating voltage and beam current have to be accurately known and the specimens should be well polished (< 0.1 μm), flat and at 90° to the beam. If the specimen is covered with a coating layer, its effect on the measured X-ray data should be accounted for [28]. Pouchou and Pichoir also used the *k*-ratios measured by Bastin and Heijligers to derive their own MACs [27]. MACs have been obtained from EPMA measurements by other authors using XMAC [28, 29-31] as well other calculation strategies [32-35]. More recently, Moy and Fournelle have implemented the option of determining MACs from EPMA measurements in their publicly available thin-film programme BADGERFILM [18].

Figure 1a shows the relative X-ray intensities for O-Kα X-rays from TiO_2, as a function of accelerating voltage [36], along with the theoretical X-ray intensities predicted by XPP that best match the measurements, which yield μ/ρ = 19,655 cm^2/g. The sensitivity of the emerging X-ray intensity to changes in μ/ρ is illustrated in Fig. 1b, which shows the results of modelling the relative X-ray intensity of O-Kα X-rays in UO_2 with XPP using μ/ρ-values of 9,990 and 12,210 cm^2/g, corresponding to a ± 10 % variation of a reference value (11,100 cm^2/g) [28].

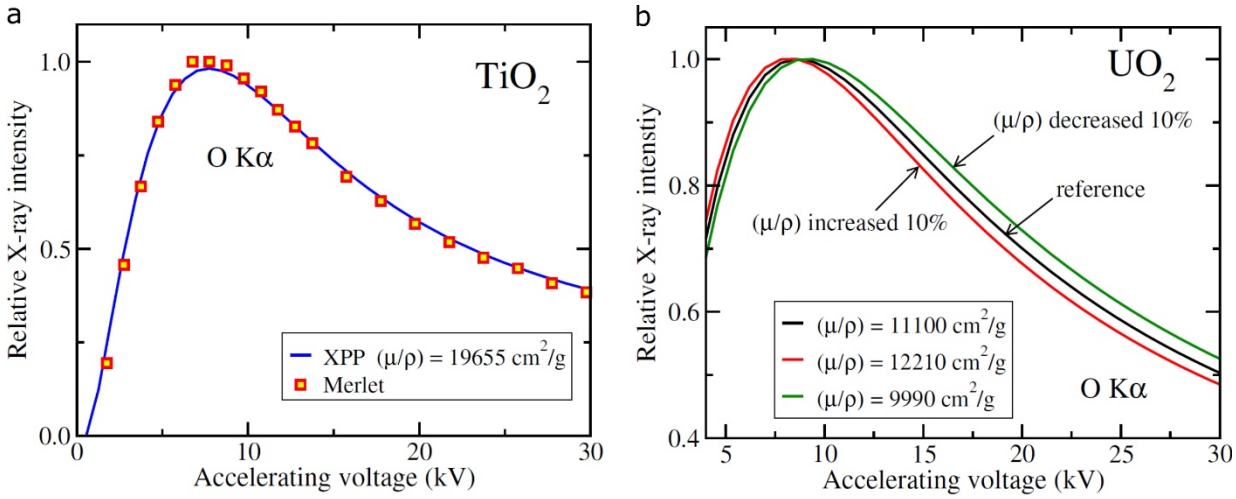

Figure 1. a) Variation of the O-Kα X-ray intensity as a function of accelerating voltage emitted from TiO_2, along with the XPP prediction for the indicated MAC value. Experimental data measured by Merlet *et al.* [36]. b) Sensitivity of energy-dependence of X-ray intensity to mass absorption coefficient.

Lurio *et al.* [37] obtained the MACs for B-Kα and C-Kα X-rays in a number of materials from particle-induced X-ray emission (PIXE) measurements. In their experiments, a film of the absorber element was placed on top of a substrate, and the X-ray intensity emitted from the substrate by proton bombardment was measured.

5. *LIGHT ELEMENTS BE, B, C, N, O, AND F*

To assess the accuracy levels in existing MAC datasets for the K-lines of the ultra-light elements, Llovet *et al.* [11] compared tabulated MACs with experimental data obtained from photo-absorption measurements, as well as from EPMA and PIXE measurements. Figure 2 compares, on logarithmic scale, the experimental MACs for Be, B, C, N, F and O emitters, as a function of absorber atomic number *Z*, with Henke82, Henke93, Heinrich86, FFAST and Sabbatucci-Salvat MACs. The experimental data include the EPMA/PIXE measurements of Bastin and Heijligers [6, 23-25], Pouchou and Pichoir [26], Lurio et al. [37] and Pöml and Llovet [28] and the photo-absorption measurements tabulated in [19] as well as those reported by Ménesguen *et al.* [20, 38, 39].

In general, the variation of the MAC with *Z* of the absorber shows several discontinuities, which correspond to the K-, L-, M- and N-edges of the absorbing elements. The discontinuities are sharp for the K- and L-edges (lower absorber *Z*) and become wider for the M- and N-edges (higher absorber *Z*). There are 49 emitter-absorber pairs for which two or more experimental MAC values exist. In these cases, the average difference between the MACs amounts to ~ 13 %. Although there are some exceptions, where larger differences between the different experimental data are observed (see below), this 13 % degree of agreement between the different experimental

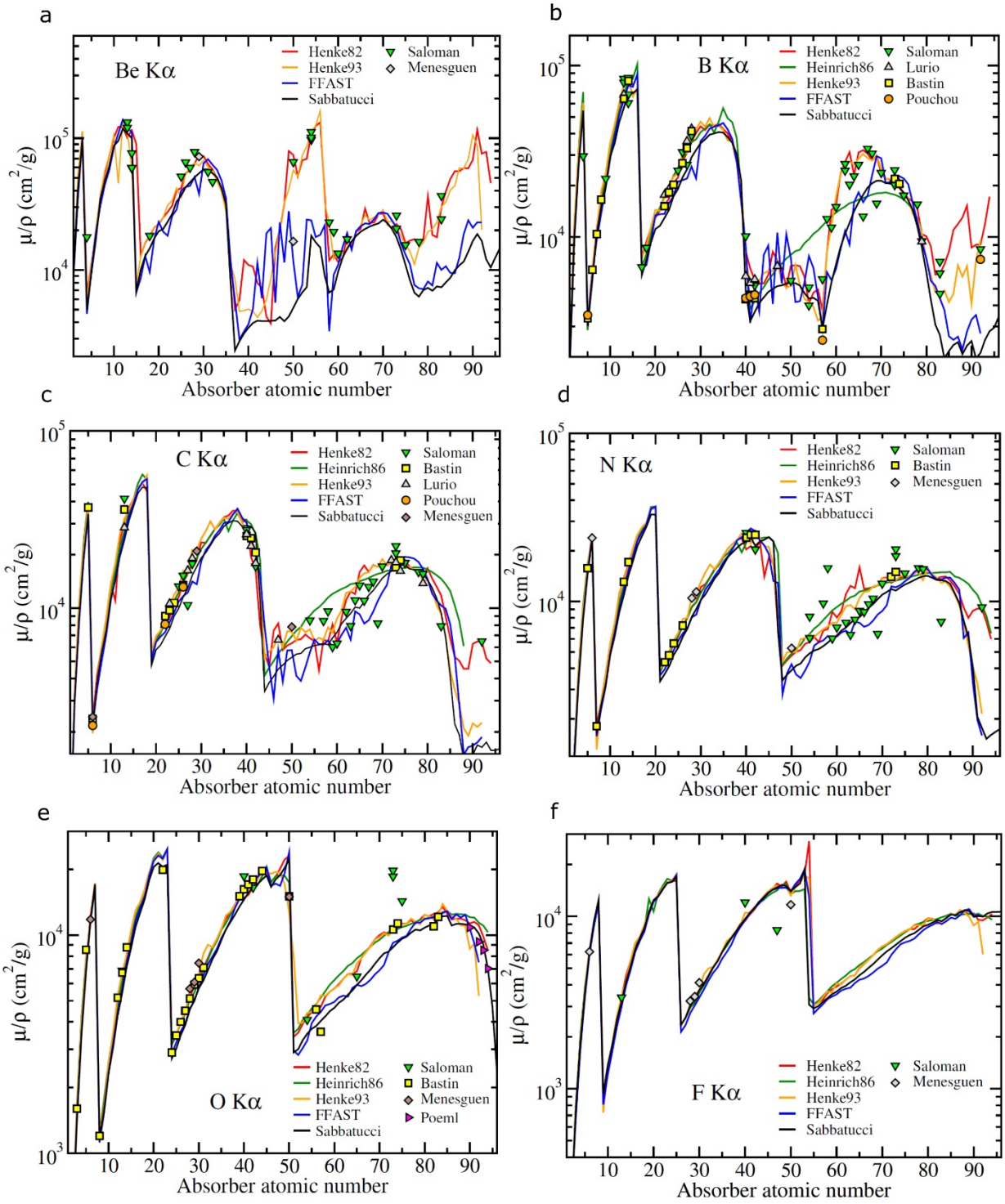

Figure 2. Tabulated (solid lines) and measured (symbols) MACs for a) Be, b) B),c) C, d) N, e) O, and f) F Kα-lines as a function of absorber atomic number.

values for the same absorber-emitter pairs is considered to be satisfactory given the difficulties of these measurements. Some of the experimental values fall outside a band that would include all the tabulated MACs, especially for *i*) N and O emitters and *ii*) absorbers with Z = 40 - 50.

These values are most likely affected by uncertainties much larger than those claimed by the authors.

Figure 2 reveals significant discrepancies between the different MAC tabulations. The differences are larger for absorbers with Z greater than ~ 40 - 50 (i.e., above the M-edges of the absorbers), where the (μ/ρ) versus Z-curves follow a rather non-smooth pattern, especially for Be and B. The disagreement is especially noteworthy for actinide absorbers (see below). Interestingly, the differences observed between the different MAC datasets decrease with Z of the emitter element, becoming less significant for O ($Z = 8$). In some cases, clear inconsistencies are observed. For instance, for Be and absorber elements around $Z = 50$, Henke82 and Henke93 MACs are consistent with Saloman *et al.*'s data, but they are in clear disagreement with the recent measurement of Ménesguen *et al.* [39], which is in very good agreement with the FFAST predictions.

The cases where tabulated values significantly disagree with the experimental data often pertain to X-ray lines located close to or between absorption edges of the absorbers. Two examples are shown in Fig. 3, which correspond to the absorption of Be (Fig. 3a) and O (Fig. 3b) Kα-lines in Sn. In the first case (Fig. 3a), the two sets of available experimental data largely disagree with each other around the Be Kα-line, which is located between the Sn N_1- and N_2-edges. The measurements listed in Saloman *et al.*'s compilation generally consist of a few energy points, in comparison with the much higher resolution measurements of Ménesguen *et al.* [20, 38, 39]. The differences between Saloman *et al.*'s data and the MACs of Ménesguen *et al.* amount up to 80 % at the Be Kα-line energy. Not surprisingly, the Henke93 MACs agree relatively well with Saloman's data, as the latter were most likely used by Henke and co-workers to produce their semi-empirical tabulation. In contrast, the differences between Saloman *et al.*'s data and the theoretical FFAST and Sabbatucci-Salvat MACs (at Be Kα-line energy) are as high as 82 % and 92%, respectively.

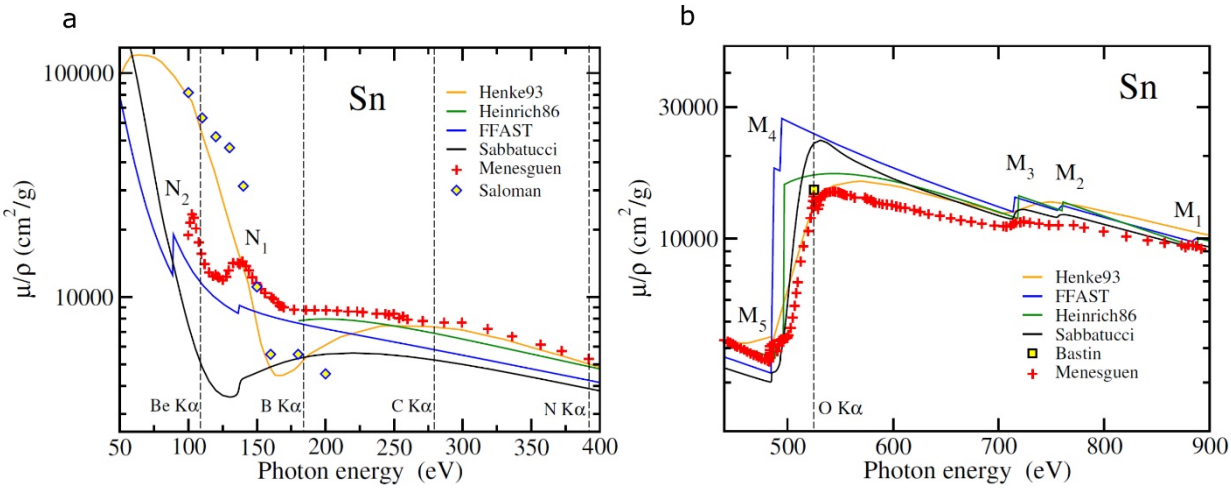

Figure 3. Tabulated (solid lines) and measured (symbols) MACs of Sn as a function of photon energy in the photon range a) 50 - 400 eV, and b) 450 - 900 eV.

Interestingly, the theoretical FFAST and Sabbatucci-Salvat MACs show a much better agreement with the recent measurements of Ménesguen *et al.*, although differences are still significant for Sabbatucci-Salvat MACs. Conversely, the latter MACs are seen to be in very good agreement with the experimental data of Saloman *et al.* (as well as with Henke93's MACs) for B. Heinrich86 MACs consistently provides the closest match to Ménesguen *et al.*'s measurements at the energies of the B-, C- and N-Kα X-rays. It is clear that further work is required to resolve these kind of inconsistencies. While undertaking high-resolution photo-absorption measurements is not without its difficulties, less complicated EPMA measurements could help resolve these discrepancies.

Figure 3b compares experimental and tabulated MACs of Sn around the energy of the O Kα-line, which is located between the Sn $M_{4;5}$ and the M_3 edges. While the FFAST MACs show sharp discontinuities at the edge positions, the Sabbatucci-Salvat MACs are smoother across the edges, resembling an experimental measurement. At the O Kα-line energy, the good agreement between the MAC measured by Bastin and Heijligers [6] and the measurements of Ménesguen *et al.* [39] is worth noting. Henke93 and Heinrich98 tabulated values agree within ~ 15 %, with Bastin's data, but the theoretical Sabbatucci-Salvat and FFAST MACs overestimate the experimental data by 47 % and 59 %, respectively. The value listed in Henke82 compilation is also off by 53 % from Bastin's value. The agreement between the MACs obtained from EPMA measurements and those obtained from photo-absorption measurements is worth noting.

A quantitative assessment of the MAC datasets can be made by calculating the root-mean-square percentage deviation, RMS, of the tabulated MACs from the corresponding experimental values. The RMS parameter is defined as follows:

$$RMS = \sqrt{\frac{1}{N}\sum_{i=1}^{N}(\Delta_i)^2}, \quad \text{with} \quad \Delta_i = \frac{(\mu/\rho)_{\text{tab}} - (\mu/\rho)_{\text{exp}}}{(\mu/\rho)_{\text{exp}}} \times 100 \qquad (6)$$

where N is the number of data points and Δ_i is the percentage deviation of a tabulated MAC, $(\mu/\rho)_{\text{tab}}$, from the experimental value, $(\mu/\rho)_{\text{exp}}$. We note that the Heinrich86 tabulation does not list values for several X-ray lines located near absorption edges. For example, there is no value for B-Kα in Zr (the B Kα-line, with energy 183.3 eV, lies near the Zr M_4 edge at 181.1 eV). In contrast, other tabulations include MAC values in these cases, but their accuracy may be questionable. For example, the MACs listed in Henke82, Henke93 and FFAST tabulations for B in Zr differ by 91 %, 67 % and 107 %, respectively, from the experimental value measured by Bastin and Heijligers [23]. This somehow penalises the RMS for the latter tabulations leaving unaffected that of Heinrich86.

RMS values of tabulated MACs from experimental values, calculated for the different emitters (Be, B, C, N, O and F) are listed in Table 1 [11]. Considering all the elements together, Henke93 provides the lowest RMS value (30.0 %) as compared to the other tabulations, followed closely by Sabbatucci-Salvat, with a RMS value of 30.6 %. While more experimental work is necessary

to draw a definite conclusion, especially for high-Z absorbers, our results seem to favour the semi-empirical Henke93 and the theoretical Sabbatucci-Salvat MACs over the other considered tabulations.

Table 1. Percentage deviation (RMS (%)) of tabulated MACs from experimental values for each emitter element (N is the number of data points). The lowest RMS values of each raw are highlighted in grey.

Element	Henke82		Heinrich86		Henke93		FFAST		Sabbatucci	
	$RMS(\%)$	N	$RMS(\%)$	N	$RMS(\%)$	N	$RMS(\%)$	N	$RMS(\%)$	N
Be	73.6	29	-	-	49.9	29	52.9	29	53.1	29
B	29.0	84	57.7	75	26.1	84	36.2	84	30.50	84
C	23.4	61	31.5	60	23.6	61	21.3	61	23.9	61
N	30.3	42	28.3	42	34.3	42	28.0	42	28.2	42
O	17.9	43	17.4	43	21.8	41	21.7	41	19.1	43
F	32.5	8	26.9	8	29.7	8	30.0	8	27.5	8
All	34.7	267	39.8	228	30.0	265	32.4	265	30.6	267

5.1. Light-element emitters (B, C, N, O) in actinide absorbers

Figure 4 shows the MACs for B-, C-, N- and O-Kα in actinide absorbers listed in Henke82, Henke93, Heinrich86, FFAST and Farthing-Walker tabulations as well as those values obtained from the Sabbatucci-Salvat photo-absorption cross-sections [15]. Farthing and Walker's tabulation is currently used in most nuclear laboratories and was produced by extrapolating Heinrich86's MACs up to $Z = 96$ [40].

For B-, C- and N-Kα there are significant discrepancies between the different tabulations. Except for B-Kα in U, the Henke93, FFAST and Sabbatucci-Salvat MACs show a good agreement with each other, with values in general much lower than the other tabulations. There is a good agreement between Farthing-Walker, Heinrich86 and Henke82 MACs for N-Kα and O-Kα. Note that both Heinrich96 and Farthing-Walker datasets do not include data for B- and C-Kα. In the case of B X-rays in U, Fig. 4a also includes the experimental MAC obtained by Pouchou and Pichoir [26] as well as that extracted from the photo-absorption measurements of del Grande *et al.* [41]. It is worth pointing out that the MAC obtained from EPMA measurements is consistent with that obtained from photo-absorption measurements. The lack of agreement between the FFAST or the Sabbatucci-Salvat MACs with the experimental data can be in part due to the long tail of the uranium 5d-5f resonance, a broad absorption feature at ~ 115 eV [41], which is neglected in atomic calculations.

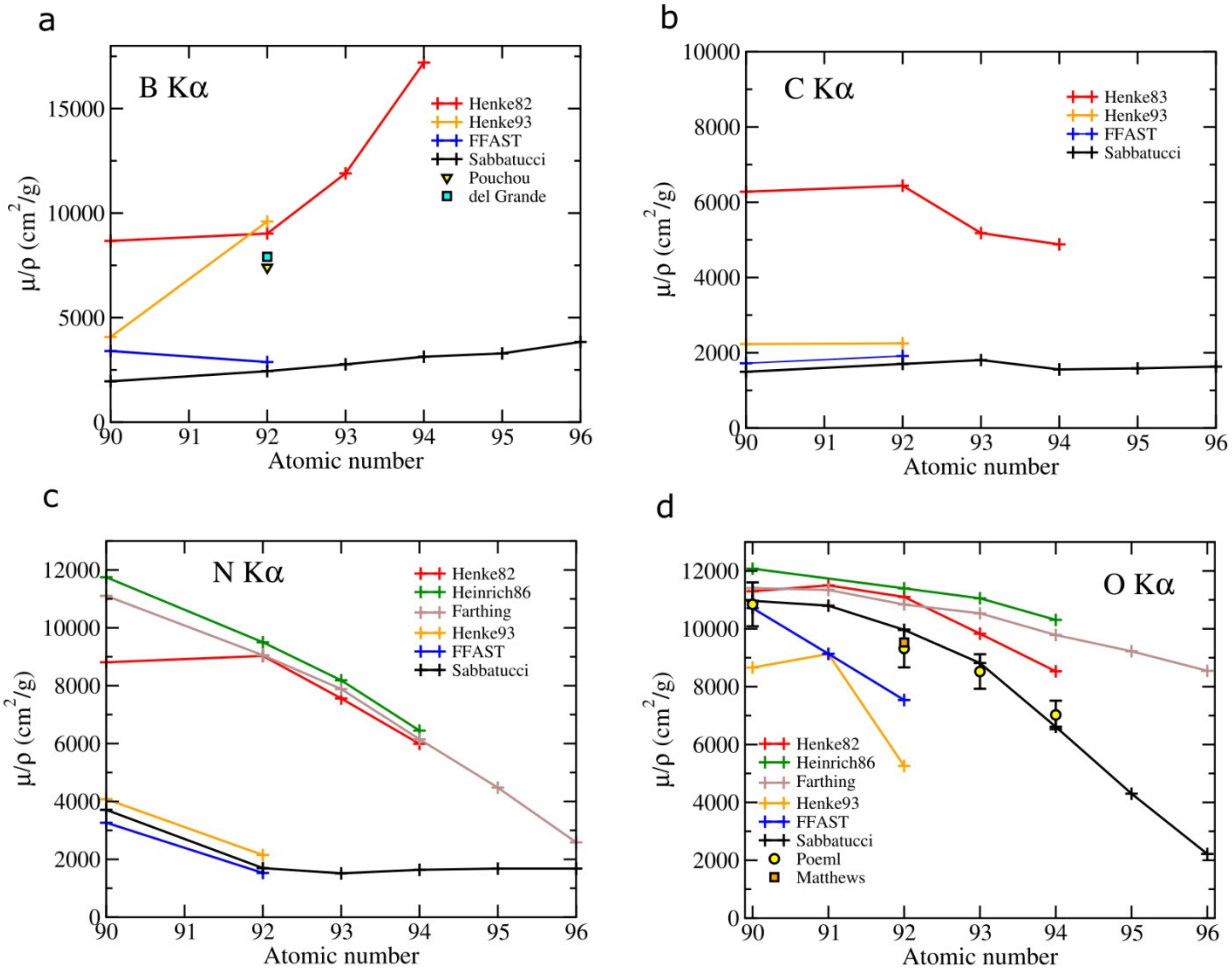

Figure 4. Tabulated (crosses joined by solid lines) and experimental (symbols) MACs for a) B, b) C, c) N, and d) O Kα X-rays as a function of absorber atomic number.

In the case of O-Kα, the discrepancies between the different MAC tabulations are smaller (except for high-*Z* absorbers) but still important for practical applications. Figure 4 also includes the experimental MACs determined by Pöml and Llovet [28] and Matthews *et al.* for U [35]. The experimental data show a consistent agreement, within the experimental uncertainties, with Sabbatucci-Salvat MACs, which would favour the use of this dataset for Am and Cm as well. In contrast, the MACs from Henke82 and Farthing tabulations are systematically higher than the experimental data, while the MACs from the Henke93 tabulation appear to be much lower than the experimental data. The FFAST MACs agree with the measured value for Th but underestimate by ~ 10 % the experimental results for U.

Pöml and Llovet [28] applied these results to improve the analysis of an uranium-doped americium oxide sample, which also contained Np and Pu. This kind of material has recently gained interest as a radioisotope heater unit for space missions into deep space, where energy from the sun is not available, because it offers better properties than the conventional pure americium oxide [42]. Table 2 compares the EPMA concentrations obtained by using

Farthing--Walker MACs for O-Kα in U, Np, Pu, and Am with those obtained using Sabbatucci-Salvat MACs (for consistency, in both cases, the same MACs were used for the rest of X-ray lines and absorbers). Significantly different estimates of the oxygen abundance were obtained, which differ nearly by ~ 50 %. The closeness of the analytical total to 100 % for the composition obtained using Sabbatucci-Salvat MACs and its agreement with thermogravimetric analysis [42] suggested a more reliable estimate of the oxygen abundance, providing further evidence of the accuracy of Sabbatucci-Salvat MACs for actinide absorbers.

Table 2. Comparison of EPMA analyses using MACs for O-Kα X-rays from different sources. From [28].

MAC source	U (wt.%)	Np (wt.%)	Pu (wt.%)	Am (wt.%)	O (wt.%)	Total
Farthing-Walker	11.2	5.01	1.57	72.2	17.1	107.2
Sabbatucci-Salvat	11.0	5.02	1.55	71.2	10.3	99.1

6. *TRANSITION METAL L-LINES*

Figure 5a compares the MACs for the Lα-lines of transition metals from Henke82, Henke93, Heinrich86, FFAST and Sabbatucci-Salvat tabulations, with the experimental data of Pouchou and Pichoir [26] and of Kyser [22], as well as with the MAC values extracted from the photo-absorption measurements of Ménesguen *et al.* [38] and of Sokaras *et al.* [43]. The experimental MACs obtained from different EPMA based methods agree reasonably well with each other (except for Ti, where the value reported by Pouchou and Pichoir [26] differs by ~ 20 % from that reported by Kyser [22]), and also with the photo-absorption measurements of Sokaras *et al.* [43] and of Ménesguen *et al.* [38].

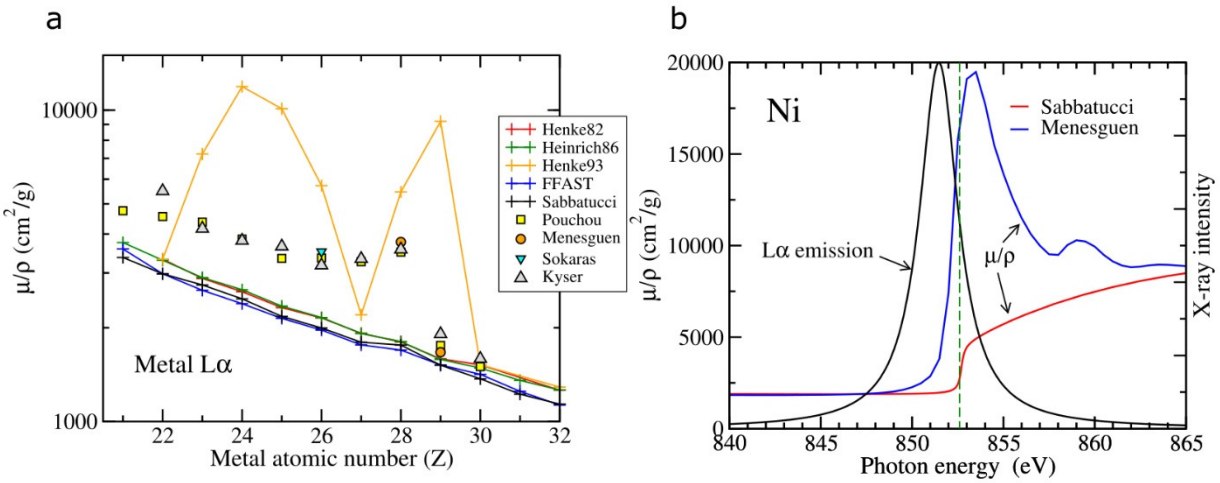

Figure 5. a) Tabulated (crosses joined with solid lines) and experimental (symbols) MACs for Lα X-rays of transition metals, as a function of metal atomic number. b) Theoretical (Sabatucci) and experimental (Ménesguen) MACs of metallic Ni around the L_3-edge (green dashed vertical line). The Ni Lα-line emission line is also shown in arbitrary scale.

For all elements except Cu and Zn, the tabulated MACs consistently underestimate the experimental data by ~ 30 - 40 %, which represents a significant source of error for EPMA analysis [30, 31] (surprisingly the MACs from Henke93 tabulation are markedly much higher than the rest of tabulations, except for Ti, Co and Zn).

The reason for this systematic underestimation arises from the near-edge structure of the $L_{2,3}$ absorption edges of the first-raw transition metals. This structure, which consist of one or several absorption peaks (also referred to as white lines), originate from electron transitions between the 2p level and the unoccupied 3d states. The near-edge structure at the Ni L_3 edge is shown in Fig. 5b, which compares the experimental MACs of Ni metal obtained by Ménesguen *et al.* [38] with the theoretical MACs of Sabbatucci and Salvat [15]. The latter calculations do not predict any absorption peak as they apply to free atoms and thus solid state effects are neglected. Because of the proximity of the Lα-line (also shown in the figure) to the L_3 absorption edge (green dashed line), the MAC at the Ni Lα-line (851.47 eV) is almost a factor 2 higher than the calculated value. Away from the edge (say below ~ 850 eV and above ~ 865 eV) there is a good agreement between Sabbatucci-Salvat MACs and the experimental data. In contrast to Ni, the experimental absorption spectrum of metallic Cu shows a typical step-like profile, with some oscillations above the edge [44]. The lack of absorption peaks stems from the fact that Cu has no unoccupied 3d states, as can be deduced from its electronic configuration [Ar]: $4s^1\ 3d^{10}$. As a result, there is a good agreement between tabulated and measured MACs, as can be seen in Fig. 5a. While this is also the case for Cu^+-compounds, the electronic configuration of Cu^{2+}-compounds ([Ar]: $3d^9$) indicates that the latter have unfilled 3d orbitals and thus they are also likely to exhibit absorption peaks at the L_3-edge [45].

Figure 5b also shows that the L_3-edge extends in part over the Lα emission line, which is represented by a Lorentzian distribution of width 2.58 eV [44]. Because $(\mu/\rho)(E)$ increases rapidly across the Lα-line width, the high-energy side of the Lα-line will be more attenuated than its low-energy side, producing a distortion to the line shape. This distortion, which depends on the excitation conditions, is known as self-absorption [46]. Note that if the MAC varies smoothly over the line width, as it is generally the case, self-absorption will only modify the line intensity but not its shape. Because the MAC is almost constant across the emission line in the case of metallic Cu [44], very little distortion to the X-ray shape line is expected.

The effect of self-absorption is an additional source of uncertainty affecting matrix corrections, since they assume that X-ray lines are narrow and MACs are simply evaluated at the line energies. By introducing a Lorentzian profile $L(E)$ to describe the X-ray line shapes and by using experimental $(\mu/\rho)(E)$-curves from high-resolution measurements, Llovet *et al.* [44] showed that analytical errors of up to ~ 9 % can be made in neglecting self-absorption, even if the MAC is accurately known at the line energy. Llovet *et al.* also showed that, when self-absorption is significant, the use of MACs determined from EPMA data may significantly reduce the analytical error. This is because the EPMA measured MAC actually represents an "effective" value that naturally accounts for the MAC variation over the line width. As a result, X-ray intensities calculated by matrix corrections match better the measured ones.

The troublesome point of the L_3 near-edge structure for EPMA analysis is that it is sensitive to the chemical state of an element. This feature is exploited by the X-ray absorption near-edge structure (XANES) technique, which gives information about the local structure around the absorbing atom as well as its oxidation state and bonding characteristics. Figure 6a compares the absorption spectrum of metallic Ni with that of NiAl [38, 48]. Due to the near edge structure, the MAC of NiAl at the Ni-Lα line energy is smaller than that of Ni, as was shown by Pouchou, who measured the MAC for Ni-Lα in γ'-Ni_3Al (12.5 wt% Al), β-NiAl (30.9 wt% Al) and metallic Ni [4] (see also [49]). Pouchou's results are displayed in Fig. 6b, which shows that the MAC for Ni-Lα in Ni bonded with one Al atom is significantly lower than that for pure Ni. The reason is that the filling of the 3d states by electrons from Al reduces the intensity of the absorption peak at the L_3-edge [4]. Because, the MAC decreases linearly with Ni concentration the additivity rule (Eq. (3)) is no longer valid. The breakdown of the additivity rule for photon energies close to absorption edges has been discussed by Deslattes [50].

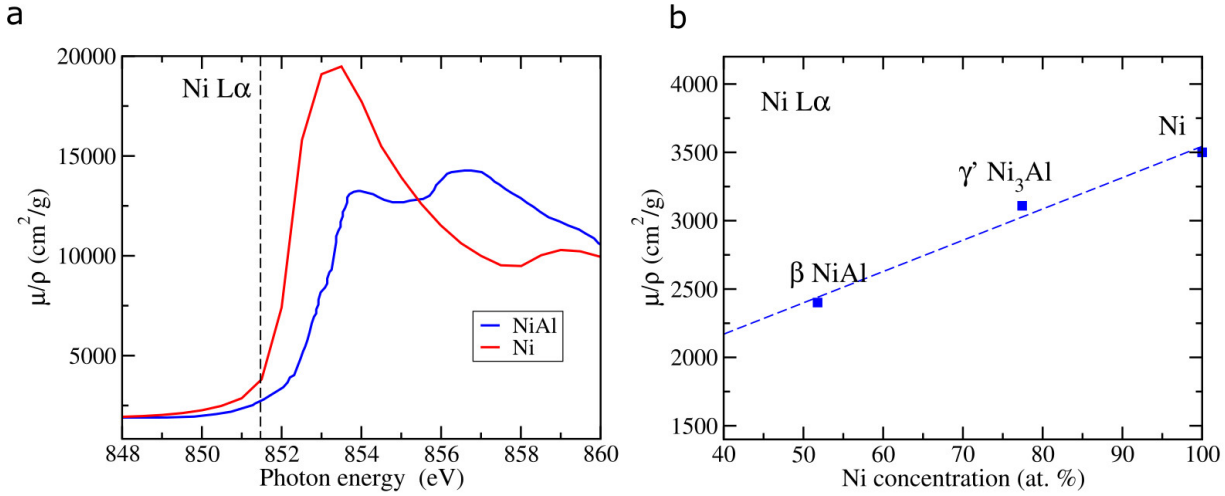

Figure 6. a) Experimental MACs of metallic Ni and NiAl around the L_3-edge (see text for details). b) EPMA measured MACs for Ni-Lα X-rays in Ni metal and in Ni-aluminides [49].

Llovet *et al.* [31] showed a similar behaviour in the case of Ni-silicides [31]. In this case, the authors demonstrated the structure of the MAC near the edge by means of self-absorption spectra. Self-absorption spectroscopy, which was developed as an alternative to conventional X-ray absorption spectroscopy [47], is based on the fact that the point-by-point intensity ratio of two L emission spectra $I_1(E)$ and $I_2(E)$, measured at two different beam energies, yields a curve which resembles the conventional X-ray absorption spectrum [44]. In spite of the much lower spectral resolution, the self-absorption spectra showed significant differences between the different Ni-silicides, pointing to changes in the occupancies of the Ni 3d states due to bonding with Si. The MACs for Ni-Lα X-rays of Ni-silicides obtained by Llovet *et al.* also showed a linear dependence on Ni concentration. These results, along with those reported by Pouchou

[49], suggest that a bonding correction is needed in Eq. (3) to calculate the MACs of transition-metal aluminides and silicides (and most likely of other transition-metal compounds).

Another situation where MACs may be affected by large uncertainties is when the emission line is located at up to a few hundred electron volts above the absorption edge [51]. The study of this region is the basis of the extended X-ray absorption fine structure (EXAFS) technique, which gives information about the local environment of an atom. In this region, the MAC shows some oscillations, which are the result of the interaction between the ejected photoelectron and other atoms surrounding the excited atom, as are observed in the absorption spectrum of Cu metal measured by Ménesguen *et al.* [20] (Fig. 7a). Because atomic photo-absorption calculations assume that atoms in the solid state interact with radiation as if they were isolated atoms, EXAFS oscillations are neglected (Fig. 7a). MAC tabulations also ignore variations near absorption edges, as mentioned earlier. The experimental MAC measured by Pouchou and Pichoir [26] for the Lβ$_1$-line slightly overestimates the measured value by Ménesguen *et al.* at the Lβ-line energy (Fig. 7a). As noted earlier, a MAC obtained from EPMA measurements represents an effective value of $(\mu/\rho)(E)$ over the width of the emission X-ray line, which could in part explain this small deviation.

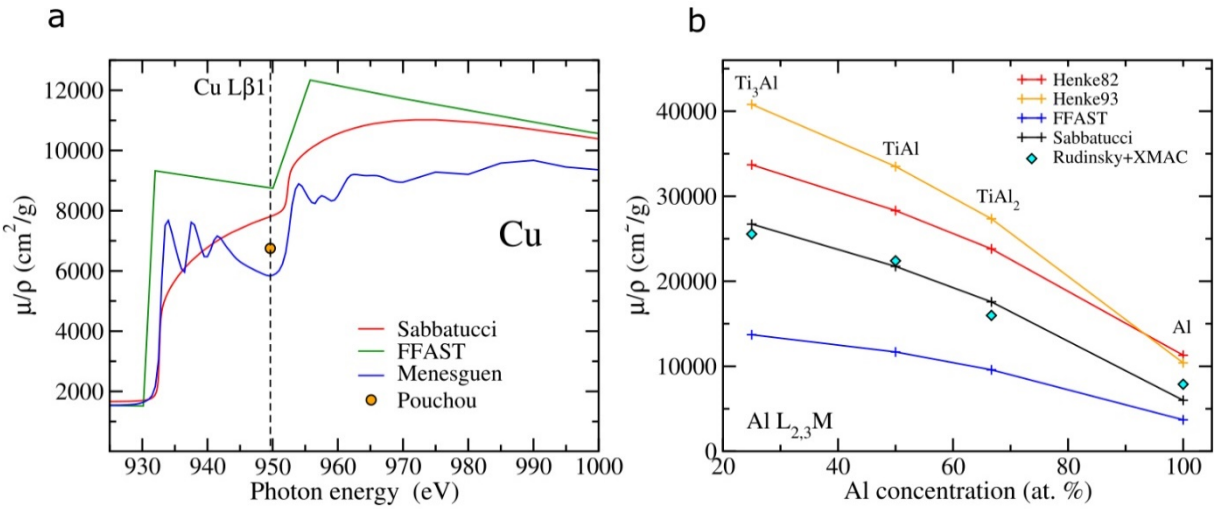

Figure 7. a) Theoretical (lines) and experimental (symbol) MACs of metallic Cu around the Cu Lβ$_1$-line (EXAFS region). b) Tabulated (crosses joined with solid lines) and measured (experimental) compound MACs for Al L$_{2,3}$M X-rays in Ti-Al compounds and Al metal, as a function of Al concentration.

7. ULTRA SOFT X-RAYS

Although most MAC tabulations (except that of Heinrich) cover the energy range above 50 eV, the accuracy of MACs below 100 eV is open to question mainly because of the scarcity of experimental data. Recently, Rudinsky *et al.* [34] measured the MACs of Al L$_{2,3}$M X-rays

(72.4 eV) in different TiAl alloys using a soft X-ray emission spectrometer (SXES). The MACs obtained by Rudinsky *et al.* were found to be in significant disagreement with the FFAST MACs and the discrepancies were attributed to missing contributions from Auger and Coster-Kronig transitions, as well as to uncertainties in some of the fundamental quantities adopted in their X-ray emission calculations [34]. Llovet *et al.* [11] re-processed the X-ray intensities measured by Rudinsky *et al.* using both XMAC and BADGERFILM, obtaining MACs in large disagreement with those reported by Rudinsky. In Fig. 7b, the MACs obtained by Llovet *et al.* [11] are compared to MACs calculated based on data extracted from the Henke82, Henke93, FFAST and Sabbatucci-Salvat tabulations for Al and three Ti-Al alloys. While the MACs from the different tabulations significantly disagree with each other, those obtained by re-processing Rudinsky *et al.*'s data with XMAC match notably well the theoretical predictions of Sabbatucci and Salvat. More systematic EPMA measurements using the SXES would be desirable to improve our understanding of MACs for ultra soft X-rays.

7. CONCLUSIONS

An assessment of the accuracy levels in MAC tabulations for soft X-rays has been presented by comparing tabulated MACs with experimental data available in the literature. The latter included both photo-absorption cross-section measurements as well as MACs obtained from EPMA and PIXE measurements. Although the 1993 semi-empirical MAC compilation of Henke *et al.* [10] provides the lowest RMS value as compared to the other tabulations for the light elements (Be, B, C, N, O, and F), the MACs obtained from the theoretical photo-absorption calculations of Sabbatucci and Salvat [15] perform better than the rest of considered tabulations when the L-lines of transition metals are also included. Uncertainties in the MAC tabulations for not including variations near absorption edges can be reduced by replacing tabulated MACs with those obtained from EPMA measurements, suitably processed with computer programs such as XMAC or BADGERFILM. MACs obtained in this way can also be used as the basis of bonding corrections for transition-metals compounds.

8. ACKNOWLEDGEMENTS

Financial support from the Spanish MCIN/AEI/10.13039/501100011033 (grant PID2019-105625RBC21) and the U.S. National Science Foundation (grants EAR-1337156, EAR-1554269 and EAR-1849386) is gratefully acknowledged.

9. REFERENCES

[1] Llovet X, *et al.* 2021 *Prog. Mater. Sci.* **116** 100673
[2] Fabian D J, *et al.* 1972 *Rep. Prog. Phys.* **34** 601

[3] Nagel D J 1969 *Adv. X-ray Anal.* **13** 182
[4] Pouchou J L 1996 *Mikrochimica Acta* **Suppl. 13** 30
[5] Llovet X, *et al.* 2012 *IOP Conf. Ser.: Mater. Sci. Eng.* **32** 012014
[6] Bastin G F and Heijligers H J M 1990 Quantitative electron probe microanalysis of carbon in binary carbides. [Eindhoven, The Netherlands: Eindhoven: University of Technology]
[7] Heinrich K F J 1986 in: *Proc. 11th Int. Congr. X-ray Optics and Microanalysis*. (Brown J D and Packwood R; Eds.) [London, CA: University Western Ontario] 67
[8] Veigele W J 1973 *Atom. Data Nucl. Data Tables* **5** 51
[9] Henke B L, *et al.* 1982 *Atom. Data Nucl. Data Tables* **27** 1
[10] Henke B L, *et al.* 1993 *Atom. Data Nucl. Data Tables* **54** 181
[11] Llovet X, *et al.* 2023 *Micros. Microanal.* (in press)
[12] Chantler C T 1995 *J. Phys. Chem. Ref. Data* **24** 71-643
[13] Chantler C T 2000 *J. Phys. Chem. Ref. Data* **29** 597
[14] Chantler C T, *et al.* 2005 *X-ray form factor, attenuation and scattering tables (v. 2.1)*. http://physics.nist.gov/ffast. [Gaithersburg, VA: NIST]
[15] Sabbatucci L and Salvat F 2016 *Rad. Phys. Chem.* **121** 122
[16] Llovet X and Salvat F 2017 *Microsc. Microanal.* **23** 634
[17] Ritchie N W M 2009 *Microsc. Microanal.* **15** 454-468
[18] Moy A and Fournelle J H 2021 *Micros. Microanal.* **27** 266
[19] Saloman E B, *et al.* 1988 *Atom. Data Nucl. Data Tables* **38** 1
[20] Ménesguen Y, *et al.* 2016 *Metrologia* **53** 7
[21] Donovan J J, *et al.* 2020 *Probe for EPMA v. 12.8.5. Users guide and reference*.
[22] Kyser F D 1972 in: *Proc. 6th Int. Conf. X-ray Optics and Microanalysis*. (Shinoda G, Kohra K and Ichinokawa T; Eds.) [Tokio, Japan: University Press] 147-156
[23] Bastin G F and Heijligers H J M 1997 *Quantitative electron probe microanalysis of boron in binary borides*. [Eindhoven, The Netherlands: Eindhoven: University of Technology]
[24] Bastin G F and Heijligers H J M 1988 *Quantitative electron probe microanalysis of nitrogen*. [Eindhoven, The Netherlands: Eindhoven: University of Technology]
[25] Bastin G F and Heijligers H J M 1989 *Quantitative electron probe microanalysis of oxygen*. [Eindhoven, The Netherlands: Eindhoven: University of Technology]
[26] Pouchou J L and Pichoir F 1988 Determination of mass absorption coefficients for soft X-rays by use of the electron microprobe. in: *Microbeam Analysis*. (Newbury D E; Ed.) [San Francisco, CA: San Francisco Press] 319
[27] Pouchou J L and Pichoir F 1991 Quantitative analysis of homogeneous or stratified microvolumes applying the model PAP. in: *Electron probe quantitation*. (Heinrich K F J and Newbury D E; Eds.) [New York, NY: Plenum Press] 31
[28] Pöml P and Llovet X 2020 *Micros. Microanal.* **26** 194
[29] Rickerby D G and Wäachter N 2000 *Mikrochimica Acta* **132** 157
[30] Gopon P, *et al.* 2013 *Microsc. Microanal.* **19** 1698
[31] Llovet X, *et al.* 2016 *Microsc. Microanal.* **22** 1233
[32] Mackenzie A P 1991 *Physica C* **178** 365
[33] Buse B and Kearns S 2018 *Microsc. Microanal.* **24** 1

[34] Rudinsky S, *et al.* 2020 *Microsc. Microanal.* **26** 741
[35] Matthews M, *et al.* 2021 *Microsc. Microanal.* **27** 466
[36] Merlet C, *et al.* 2003 in: *Book of Tutorials and Abstracts of the EMAS 2003 Workshop*. [Antwerp, Belgium: European Microbeam Analysis Society eV (EMAS)]
[37] Lurio A and Reuter W 1977 *J. Phys. D: Appl. Phys.* **10** 2127
[38] Ménesguen Y, *et al.* 2018 *Metrologia* **55** 56
[39] Ménesguen Y, *et al.* 2018 *X-ray Spectrom.* **47** 341
[40] Farthing I R and Walker C T 1990 *Heinrichs mass absorption coefficients (for the K, L and M X-ray lines)*. Technical Note K0290140 [Karlsruhe, DE: JRC]
[41] del Grande N K, *et al.* 1987 *J. Phys. Colloques* **48** C9-951
[42] Vigier J F, *et al.* 2018 *Inorg. Chem.* **57** 4317
[43] Sokaras D, *et al.* 2011 *Phys. Rev. A* **83** 052511
[44] Llovet X, *et al.* 2022 *Microsc. Microanal.* **28** 123
[45] Koster A S 1973 *Mol. Phys.* **23** 625
[46] Liefeld R J 1968 Soft X-ray emission spectra at threshold excitation. in: *Soft X-ray band spectra and the electronic structure of metals and materials*. (Fabian D H; Ed.) [New York, NY: Academic Press] 133
[47] Burgäzy F, *et al.* 1989 *Z. Naturforsch.* **44**a 180
[48] Pease D and Azároff L V 1979 *J. Appl. Phys.* **50** 6605
[49] Pouchou J L and Pichoir F 1985 *J. Microsc. Spectrosc. Electron.* **10** 291
[50] Deslattes R D 1969 *Acta Cryst. A* **25** 89-93
[51] Nagel D 1968 Absorption edge effects in electron probe microanalysis. in: *Quantitative electron probe microanalysis*. (Heinrich K J H; Ed.) [Washington DC: National Bureau of Standards]